A normal *gem*-dimethyl effect in the base-catalyzed cyclization of ω-(*p*-nitrophenyl)hydantoic acids: evidence for hindered proton transfer in the permethylated esters †

Iva B. Blagoeva,[a] Anthony J. Kirby,[b] Ivaylo I. Kochiyashki,[a] Asen H. Koedjikov,[a] Ivan G. Pojarlieff[a] and Maria M. Toteva[a]

[a] *Institute of Organic Chemistry, Bulgarian Academy of Sciences, and ul. Acad. G. Bonchev block 9, Sofia 1113, Bulgaria. E-mail: ipojarli@orgchm.bas.bg*
[b] *University Chemical Laboratory, Cambridge, UK CB2 1EW*

Received (in Cambridge, UK) 21st March 2000, Accepted 23rd June 2000
Published on the Web 15th August 2000

The cyclization of hydantoic acids **2-UA** and **3-UA** – kinetics, solvent kinetic isotope effects (SKIE) and buffer catalysis – were studied in an attempt to explain the disappearance of the *gem*-dimethyl effect (GDME) in the specific base-catalyzed cyclization of hydantoic esters. pH-Rate profiles for both acids (after correction for ionization and for reversibility at high pH) show two regions of unit slope corresponding to different mechanisms. For **2-UA** at high pH and **3-UA** at lower pH the mechanism is considered to involve rate-determining attack by the ureido anion on the neutral carboxy group, consistent with the observed inverse SKIE. The normal GDME of 15 provides strong evidence that anomalies observed with the esters do indeed result from steric hindrance to proton transfer. The change to rate determining departure of OH^- with **2-UA** is caused at low pH by acid catalysis of the reversion of the tetrahedral intermediate ($\mathbf{T}^-$) to reactants, while with **3-UA** at high pH this takes place through $\mathbf{T}^{2-}$. The GDME favours attack on the carboxylate anion but makes ring opening more difficult, thus decreasing acid inhibition. The observed $\beta = 0.44$ for general base catalysis of the cyclization of **2-UA** is consistent with concerted deprotonation and attack of the ureido group. With **3-UA** two simultaneous general base-catalyzed reactions take place: slow deprotonation of the ureido group ($\beta = 1.0$) and attack of the ureide anion on the carboxy anion aided by the buffer conjugate acid. The estimated GDME is 2800 for the equilibrium between acid anion and hydantoin,‡ but only 45 and 15 for catalysis by H_3O^+ and OH^-, respectively: both reactions are presumed to go through early transition states.

A convenient way to accelerate the bioorganic reactions of small molecules is to introduce steric strain into the substrate. In cyclization reactions this is readily done by introducing substituents into the interconnecting chain: the resulting increase in rate defines the *gem*-dimethyl effect (GDME).[1] However, in a recent study[2,3] of catalytic mechanisms for the ring closure of hydantoic esters, we found no GDME for the base-catalyzed reaction. We concluded that the rate determining step had changed, for the most heavily substituted compounds, from the formation of the tetrahedral intermediate to its breakdown, because of steric hindrance in proton transfer to the leaving ethoxy group. In the tetrahedral intermediate, $\mathbf{T}^-$, the two

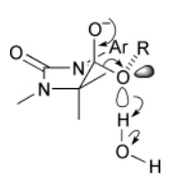

$\mathbf{T}^-$

methyl groups screen one side and the *N*-aryl substituent the other, while R (ethyl was studied) in its least hindered conformation blocks easy access of a general acid. If this analysis is correct, and the effect depends on steric hindrance in proton transfer to the developing ethoxide by its ethyl group, it should be reduced or removed if a smaller group replaces ethyl. We have tested this proposition by studying the cyclization of the hydantoic acids shown in Scheme 1.

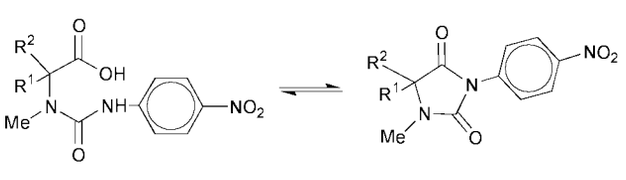

UA H

	R^1	R^2
1	H	H
2	Me	H
3	Me	Me

Scheme 1

We find that hydantoic acids **2** and **3** undergo base-catalyzed ring closure more slowly than the esters when the pH is higher than the p*K* of the COOH group; and that the results confirm our prediction. The hydroxide-catalyzed cyclization of the fully methylated acid **3-UA** shows a normal GDME, and the solvent kinetic isotope effects (SKIE) suggest that acids **2-UA** and **3-UA** are cyclized by the same mechanism.

Experimental

Materials

Inorganic reagents and buffer components were of analytical

† Pseudo-first-order rate constants are available as supplementary data. For direct electronic access see http://www.rsc.org/suppdata/p2/b0/b002276o

‡ The IUPAC name for hydantoin is imidazolidine-2,4-dione.

DOI: 10.1039/b002276o

grade and used without further purification. Potassium hydroxide and buffer solutions were prepared with CO_2-free distilled water. D_2O, 99 atom%, was from Aldrich. 1-Methyl-3-(4-nitrophenyl)hydantoin and its 2-methyl- and 2,2-dimethyl-derivatives have been described previously.[4]

p*K* Determination for ureido acids 1-UA and 2-UA

This was done by potentiometric titration using a Radiometer pH M 84 Research pH-meter equipped with a GK 2401 C electrode standardized at pH 6.87, 4.01 and 9.18, respectively. In a 50 ml vessel thermostatted at 25.0 °C by means of a glass mantle with circulating water, 0.300 mmol of the hydantoin were completely dissolved under magnetic stirring in 15.30 ml of 1 M KOH. The vessel was covered with parafilm and nitrogen passed through an aperture. Two further apertures were made for inserting the combined electrode and the burette tip. After dissolution, the excess of KOH was neutralized with 15.00 ml of 1 M HCl and further titrated with 0.1 M HCl in ten aliquots, measuring the pH after each addition. To avoid complications due to cyclization to hydantoin, care was taken for the whole procedure, after neutralization of the excess KOH, to be completed within 4 min. The large excess of KOH made exact neutralization difficult: for this reason the p*K* values were obtained by fitting the results to eqn. (1), where the error in the added volume of 1 M HCl, *a*, was treated as an adjustable parameter.

$$pK_a = \log \frac{[C_{tot}(V_{titr} - a)/b] - 10^{-pH}}{[C_{tot}(1 - (V_{titr} - a))/b] + 10^{-pH}} + pH \quad (1)$$

In eqn. (1) C_{tot} is the total concentration of added acid, taking into account the dilution caused by titration; V_{titr} the volume of added titrant and *b* the calculated volume of titrant necessary for complete reaction.

Kinetic measurements

The cyclizations of the acids are much slower than those of the corresponding esters because of ionization of the carboxy group, so rates could be measured by conventional kinetics up to much higher pHs. Rate constants were determined at 25.0 ± 0.1 °C under pseudo-first-order conditions in the thermostatted cell compartment of a Unicam SP-800 or Carl Zeiss Jena UV–VIS spectrophotometer. The rate of cyclization of the ureido acids (**2** or **3**)-**UA** was followed by monitoring the decrease of absorbance at 330 nm: the substrate solution was prepared by mixing a 0.025 M solution of hydantoin in DMSO with 1 M KOH in a 1 : 2 (v/v) ratio. Next 30 μl of this solution was added to 2.80 ml of the preheated buffer solution, followed by 20 μl of 1 M HCl, to neutralize the excess base. Pseudo-first-order rate constants,† k_{obs}, were obtained by nonlinear-regression curve-fitting to the equation where $A_t = A_0\ e^{-k_{obs}t} + A_\infty$ where A_t, A_0, and A_∞ are the absorbances at times *t*, zero, and infinity, respectively. The ionic strength was maintained constant (1.0 M) with KCl. pH Values were measured at the end of each kinetic run.

Experiments in D_2O solutions were run simultaneously with duplicates in H_2O of the same buffer concentration in the multicell compartment of the spectrophotometer. The observed rate constants were extrapolated to zero buffer concentration to determine the isotope effect, as described in the results section. pD Values were obtained by adding 0.4 to the pH-meter readings and the a_{OD} values calculated using $pK_w = 14.86$.[5]

Product analysis

Monitoring the cyclization reaction by repetitive scanning gave good isosbestic points and spectra after ten half-lives were identical to spectra of hydantoin of the same total concentration under the same conditions. At higher pHs, where equilibria were established, the same infinity readings at 330 nm were obtained after ten half-lives starting from either the hydantoin or from the potassium salt of the acid (obtained from the hydantoin by hydrolysis at higher base concentration).

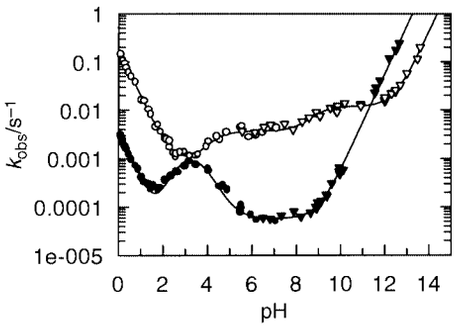

Fig. 1 Observed first order rate constants for cyclization of ureido acids **2-UA** (closed symbols) and **3-UA** (open points). Circles represent rates measured in HCl solutions or values extrapolated to zero buffer concentration. Triangles refer to data obtained in KOH solutions or 0.02 M (total) buffer solutions. Lines are drawn by means of eqns. (7) and (9).

Results

Kinetics and mechanisms

pH–Rate profiles for the cyclization of ω-(*p*-nitrophenyl)-hydantoic acids. The observed pseudo-first-order rate constants for the cyclization of the hydantoic acids are plotted as a function of pH in Fig. 1.

Data below pH 7 were obtained in HCl solutions ($a_H = 0.851$[HCl])[4] or extrapolated to zero buffer concentration. At higher pH values (7–10) the data refer to 0.02 M buffers (phosphate, TRIS, carbonate and glycine amine): we are confident that the contribution of buffer catalysis is not significant at this concentration. The high pH-region (pH > 11.52) was studied in KOH solutions and the pH taken as 14 + log [OH^-]. Under these conditions the data are derived from measurements of the reverse reactions, the hydrolysis of the hydantoins **2-H** and **3-H** (see below).

(a) 2,3-Dimethyl-5-(4-nitrophenyl)hydantoic acid ***2-UA***. As observed previously[3] with the ethyl ester of **2-UA**, the pH–rate profile shows a minimum, representing the change from acid to base catalysis, as low as pH 2. The rate profiles are closely similar at higher pHs also, when the reaction is calculated in terms of the free acid (see below). The negative slope between pH 4–6 marks the ionization of the COOH group in a region of water-catalyzed reaction of the free acid, reaction (2).

$$\mathbf{UA} \overset{K_{UA}}{\rightleftharpoons} \mathbf{UA}^- + H^+ \quad (2)$$

The dissociation constant, K_{UA}, for the carboxy group could be determined potentiometrically as 3.60 ± 0.02 when precautions were taken to avoid the facile cyclization of the acid. The plateau between pH 6–9 must be a second reaction, first-order in [OH^-]. However, the appearance of a second region of slope 1 at still higher pH is not due to a hydroxide-catalyzed cyclization of the anion (or a kinetically equivalent reaction of the free acid, second-order in [OH^-]) but arises because cyclization no longer proceeds to completion. As observed previously[4] with the cyclization of the amide of **2-UA**, the equilibrium between the anion of **UA** and the cyclic hydantoin (equilibrium (3)) becomes significant around pH 9: at the

$$\mathbf{UA}^- \overset{k_f/k_r}{\rightleftharpoons} \mathbf{H} + OH^- \quad (3)$$

highest pHs the studied cyclization is no longer observed; the observed rate constant for equilibrium (3), k_{obs}, and the equilibrium constant, K_e, are given by eqns. (4) and (5), respectively.

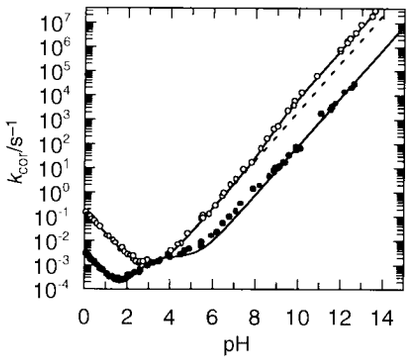

Fig. 2 pH–Rate profiles from Fig. 1, corrected for ionization and equilibrium (see the text). Closed circles represent k_{cor}, for **2-UA**, open circles data for **3-UA**. Solid lines are drawn by means of eqns. (6), (7) and (9). The dashed line is obtained from data at pH < 7 omitting the reactions associated with the carboxylate anion at high pH.

$$k_{obs} = k_f + k_r a_{OH} \quad (4)$$

$$K_e = k_f/k_r = [\mathbf{H}]a_{OH}/[\mathbf{UA}^-] \quad (5)$$

A value for $K_e = 4.44 \times 10^{-6}$ mol dm^{-3} has been determined previously[4] from spectroscopic data. The best fit of the new kinetic data gives a somewhat higher value, $(1.01 \pm 0.13) \times 10^{-5}$ mol dm^{-3}.

Fig. 2 shows the pH–rate profile for the reaction of **2-UA** corrected for ionization, using the fraction of reactant present as the free acid, **2-UA**, and for equilibration, based upon the fraction $(k_f/(k_f + k_r a_{OH}))$ of the total reaction going in the forward direction. This corrected rate constant, k_{cor}, is given by eqn. (6).

$$k_{cor} = \frac{k_{obs}(a_H + K_{UA})K_e}{a_H(K_e + a_{OH})} \quad (6)$$

As was found for the cyclization of its ethyl ester studied previously,[3] the pH–rate profile for the cyclization of **2-UA** can be described by eqn. (7). The last term accounts for ionization and equilibration (from eqns. (4) and (5)), respectively.

$$k_{obs} = k^1_H a_H + \left(\frac{k_w + k_{OH}a_{OH}}{1 + k^2_H a_h}\right)\left(\frac{a_H(K_e + a_{OH})}{(a_H + K_{UA})K_e}\right) \quad (7)$$

The rate constant k^1_H represents acid catalysis below pH 2, while the next term can be derived from Scheme 2 (R^3 = *p*-nitrophenyl) under certain limiting conditions[3] when the base A^- is either water or OH^-. The apparent constants included in this term are interpreted in the following discussion.

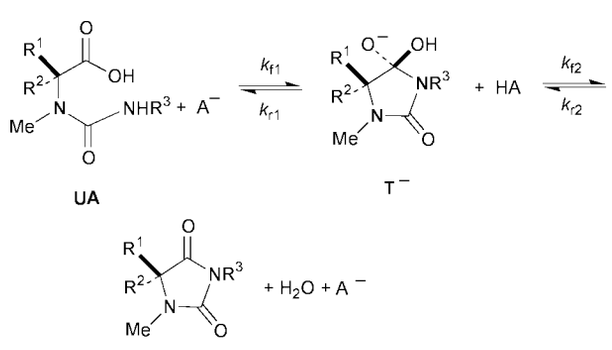

Scheme 2

The corrected rate profile for the cyclization of **2-UA** (Fig. 2), like that for its ester,[3] exhibits two regions of OH^- catalysis. The apparent rate constants, designated for greater simplicity as k^a_{OH} at lower pH and k^b_{OH} at higher pH, are separated by a pH-independent region, k_w. For the corresponding reaction of the esters the sum of the evidence, including solvent kinetic isotope effects and buffer catalysis data, led to the conclusion[3] that the rate-determining step for the k^b_{OH} reaction was the specific base-catalyzed attack of the ureide anion on the carboxylate group. k^a_{OH}, on the other hand, represented acid inhibition of the reversible formation of the negatively charged tetrahedral intermediate, $\mathbf{T}^-$, the rate determining step now being the elimination of the ethoxy group aided by proton transfer from water. The same arguments can be applied to the free acid, with OH as the leaving group in place of OEt. Relevant evidence is the inverse SKIE of 0.76 estimated for k^b_{OH} with **2-UA** (Table 2). Thus the constants of eqns. (4) and (5) and of Table 1 relate as follows to the constants of Scheme 2:§ $k^b_{OH} = k_{OH} = k_{f1OH}$, $k_w = k_{f1w}$, $k^2_H = k_{r1H}/k_{f2w}$ and $k^a_{OH} = k_w/k^2_H K_w$. The rate constants obtained by curve fitting k_{obs} to eqn. (7) are summarized in Table 1. The measured value of K_{UA} was used (Table 5), but K_e was treated as an adjustable parameter.

(b) 2,2,3-Trimethyl-5-(4-nitrophenyl)hydantoic acid ***3-UA***. As can be seen from Fig. 1, with **3-UA** the equilibrium involving the ring form begins to be significant only at pH 12, some 3 pH units higher than observed with **2-UA**. This is a result of the strong *gem*-dimethyl effect on the equilibrium. The similarity to the profile of the ester is less marked than for **2-UA**. Acid catalysis is simply first order in $[H^+]$, as opposed to the complex dependence observed with the ester.[3] Up to ph *ca*. 8, catalysis by base is first order in $[OH^-]$, the same as the ester, with the profile accurately described by eqn. (8).

$$k_{obs} = \frac{(k_H a_H + k_w + k_{OH}a_{OH})a_H}{a_H + K_{UA}} \quad (8)$$

The value of $pK_{UA} = 4.22 \pm 0.12$ was derived from the rate profile (**3-UA** cyclized too fast to allow a potentiometric titration) by fitting to eqn. (8) the data (up to pH ~7) extrapolated to zero buffer concentration. At higher pH the parameters so obtained do not fit the rate data, as can be seen from the dashed line on Fig. 2 and the second "step" in the plateau of Fig. 1. The mismatch amounts to a factor of *ca.* 3. Although buffer catalysis is stronger for the reaction of **3-UA** this "mismatch" is not due to catalysis by the 0.02 M buffers: experiments varying the total concentration of carbonate buffers showed this could account for no more than 10% of the observed rate. Rather, as has been observed before[6] in the cyclization of the *ω*-phenyl analogue of **2-UA**, the increase in rate is due to the appearance of a cyclization reaction involving the carboxylate anion, formally second order in $[OH^-]$ for the reaction of the free acid, followed by a rapid change in the rate-determining step. The reaction path is presented in Scheme 3 (R^3 = *p*-nitrophenyl).

The breakdown of $\mathbf{T}^-$ to hydantoin (**H**), k_{f_2}, is catalyzed by water acting as a general acid when $A^- = OH^-$, and is the same process as that in Scheme 2. Its reverse, the breakdown to the dianion, is a new OH^--catalyzed route. Eqn. (9) extends equation (8) to the steady state solution of Scheme 3.

$$k_{obs} = (k_H a_H + k_w)f_a + \frac{(k_{OH}a_{OH}f_a + k^A_{OH}a_{OH}f_b)(K_e + a_{OH})}{(1 + k^2_{OH}a_{OH})K_e} \quad (9)$$

Here $f_a = a_H/(a_H + K_{UA})$ is the fraction of the free acid and $f_b = K_{UA}/(a_H + K_{UA})$ is the fraction of the anion. Formally k_{OH} and k^A_{OH} represent the bimolecular rates for cyclization of the free acid and the anion respectively. The constant k^2_{OH} accounts for the change-over in rate-determining step. The change in the rate-determining step leads to the assignment of k_{OH} as the

§ Addition of w, OH, H to the subscripts of the constants of Scheme 2 denotes the cases when A^- is water, OH^- and HA is H_3O^+, respectively.

Table 1 Rate constants for H^+, OH^- and H_2O-catalysed ring closure of 5-(4-nitrophenyl)hydantoic acids at 25 °C and ionic strength 1.0 M

Compound	k^b_{OH}/dm^3 mol^{-1} s^{-1}	k^a_{OH}/dm^3 mol^{-1} s^{-1} [a]	k_w/s^{-1}	k^2_H/dm^3 mol^{-1} s^{-1}	k^1_H/dm^3 mol^{-1} s^{-1}	K_e/mol dm^{-3}
2-UA [b]	(1.45 ± 0.07) × 10^6	2.42 × 10^7	(1.90 ± 0.2) × 10^{-3}	(7.85 ± 1.32) × 10^3	(4.07 ± 0.2) × 10^{-3}	(1.03 ± 0.03) × 10^{-5}
	k_{OH}/dm^3 mol^{-1} s^{-1}	k^A_H/dm^3 mol^{-1} s^{-1}		k^2_H/dm^3 mol^{-1} s^{-1}		
3-UA [c]	(2.19 ± 0.08) × 10^7	(1.68 ± 0.47) × 10^3	(8.11 ± 1) × 10^{-4}	(1.41 ± 0.43) × 10^5	0.190 ± 0.008 [d]	(2.85 ± 0.30) × 10^{-2}

[a] $k_w/k^2_H K_w$. [b] Eqn. (7). [c] Eqns. (8) and (9), see text. [d] k_H of eqn. (8).

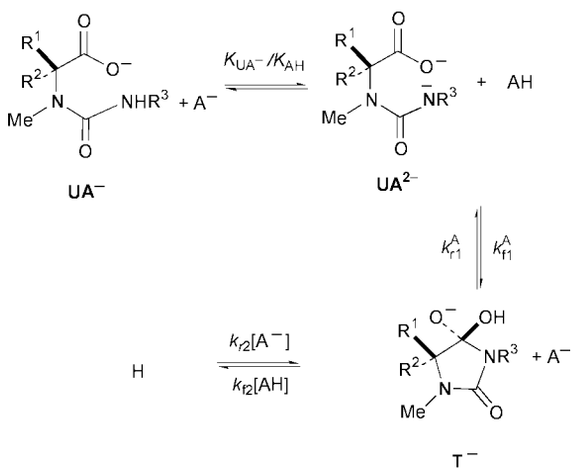

Scheme 3

OH^--catalyzed cyclization of the free acid to $\mathbf{T}^-$, defined as k_{f1OH} in Scheme 2. Similarly $k^A_{OH} = k^A_{f1}K_{UA^-}/K_w$ and $k^2_{OH} = k^A_{r1}/k_{f2}$ when A^- in Scheme 3 is OH^-. Then the observed rate on the second plateau (between pH 9–11) equals $k^A_{OH}/k^2_{OH} = 0.0119$ s^{-1}, because $k_{OH}K_w/K_{UA} \ll k^A_{OH}$. The assignment is rigorous in so far as there is no plausible mechanism for base catalysis of the expulsion of OH^- from $\mathbf{T}^-$, which would be required if k^A_{OH} was assigned to this step.

The pK_{UA^-} of **3-UA** was determined[7] as 14.51, using Yagil's acidity function H_.[8] Attempts to determine K_e independently were unsuccessful because of the strong absorbance of the dianion formed by ionization of the ureido group, $\mathbf{UA}^{2-}$. So K_e was derived from the rate data at pH 9–13.5 by means of a linear fit to eqn. (5) and the value further refined by fitting all the data to eqn. (9). There are too many unknown parameters for a one-step determination, so the constants k_H, k_w and pK_{UA}, already obtained from the fit of the data up to pH 7 to eqn. (8), were fed in as known parameters in eqn. (9). The value for k_{OH} was re-optimized, together with k^A_{OH}, k^2_{OH} and K_e, to fit the entire data set, giving the values listed in Table 1.¶

Solvent kinetic isotope effects. As attention was focused on the base-catalyzed cyclization, and particularly on the reaction presumed to be specific base catalysis of formation of the tetrahedral intermediate, SKIE were measured at pH 6.45 in cacodylate buffers (0.02–0.05 M). This pH value falls in the region of k^b_{OH} for **2-UA** and k_{OH} for **3-UA**. In both cases the rates extrapolated to zero buffer concentration are pH independent and equal to $k_{OH}K_W/K_{UA}$. The isotope effect was obtained directly from their ratio in H_2O and D_2O, respectively. The equilibrium isotope effect, K^H/K^D, of K_W/K_{UA}, where AH is a weak acid, is usually estimated to be 2.5.[9] Using this value the data in Table 2 gave a SKIE for k_{OH} of 0.76 and 0.72 for **2-UA** and of **3-UA**, respectively. This marks a significant difference from the cyclizations of the corresponding ethyl esters,[3] where inverse SKIE (0.78 and 0.6 respectively) were observed only with the esters of **1-UA** and **2-UA**, while the ester of **3-UA** showed a normal SKIE of 1.8. This is strong evidence that with the free acids no change in mechanism occurs in the fully methylated compound, and that the OH^--catalyzed reactions under discussion are specific base-catalyzed. As discussed for the esters[3] the likely mechanism for specific base catalysis involves the attack of the ureido anion on the carboxy group.

¶ The value of k_{OH} from eqn. (8) is 2.12 × 10^7 dm^{3}mol^{-1} s^{-1}.

Table 2 Kinetic solvent isotope effects, k^H/k^D, in cacodylate buffers, 0.7 fraction base, pH 6.45 at 25 °C and ionic strength 1.0 M

Compound	$k_{OH}K_w/K_{UA}$	k_{OH} (estimate)	k_{buff}
2-UA	1.9	0.76	6.4 [a]
3-UA	1.8	0.72	2.6

[a] Uncertain value because general catalysis is very weakly expressed in D_2O: the overall rate increases only 6% from 0.02 to 0.05 M buffer.

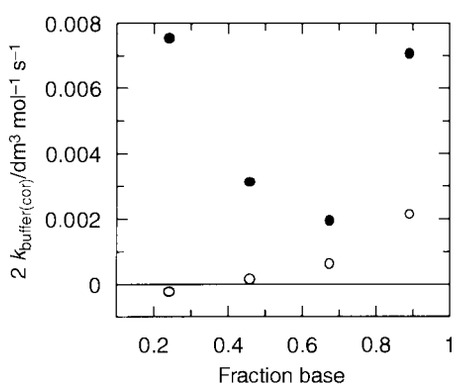

Fig. 3 Plots of $k_{buff(cor)}$ against fraction base in glycine (carboxylic acid) buffers for **2-UA** (closed circles) and **3-UA** (open circles).

General base catalysis. Buffer catalysis was studied in glycine, formate, acetate and cacodylate buffers. In glycine and the lower pH formate buffers at the concentrations used, the pH varied considerably with concentration because of "buffer failure" (significant amounts of H^+ must be provided by dissociation of the acid component of the buffer, thus changing the acid/base ratio). This was allowed for as described in ref. 2. The glycine buffers used covered a pH range of 2.2 to 3.5. For **2-UA** (Fig. 2) this is the pH region where there is a change from first to zero order in [OH^-]; it also marks the transition from acid to base catalysis for **3-UA**. This could account for the lack of linearity in the plots in Fig. 3, where $k_{buff(cor)}$ is the slope of the linear dependence of k_{obs}‖ corrected for ionization (eqn. (6), equilibrium is not important in this pH region) on [buffer] at constant fraction base.

As seen with **2-UA**, buffer catalysis is not detectable below pH 3 (in buffers more acidic than 70% free base glycine), while with **3-UA** general acid catalysis (GAC) apparently changes to general base catalysis,** in line with the changes in specific

‖ The second-order constants for buffer catalysis are calculated by omitting the data below 0.0459 M to avoid large deviations in pH and fraction base.

** Attempts to extract constants from the data yielded, however, results of very large uncertainty.

Table 3 Buffer catalysis data for the cyclization of 2,3-dimethyl-5-(4-nitrophenyl)hydantoic acid, **2-UA**, at 25.0 °C and ionic strength 1.0 M

Buffer acid	pK_{AH} [a]	Conc. range [b]/mol dm^{-3}	Fract. base	k_{A^-}/dm^3 mol^{-1} s^{-1} [b]
$H_3N^+CH_2CO_2H$	2.45	0.009–0.185	0.242	[c]
		0.009–0.185	0.459	
		0.009–0.185	0.675	
		0.009–0.185	0.892	
HCO_2H	3.57	0.01–0.2	0.3	0.029 ± 0.004 [d]
		0.01–0.2	0.5	k_{AH} = (6 ± 2)
		0.01–0.2	0.7	
		0.01–0.2	0.9	
CH_3CO_2H	4.62	0.009–0.178	0.215	0.0833 ± 0.011 [d]
		0.009–0.178	0.44	k_{AH} = (3.2 ± 1.5)
		0.009–0.178	0.664	
		0.009–0.178	0.888	
$(CH_3)AsO_2H$	6.19	0.01–0.2	0.1	0.409 ± 0.033 [e]
		0.05–0.2	0.3	
		0.05–0.2	0.5	
		0.05–0.2	0.7	
		0.05–0.2	0.9	

[a] pK_{AH} values from ref. 6. [b] Three or four runs carried out within each concentration range. [c] See text. [d] Calculated from eqn. (11). [e] Calculated from eqn. (10).

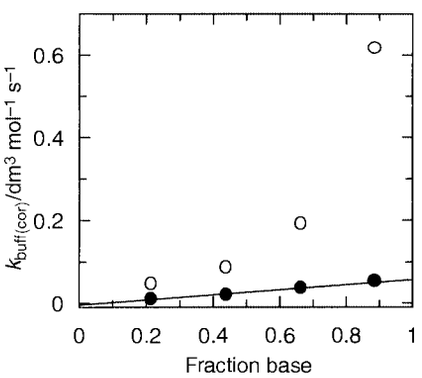

Fig. 4 Plots of $k_{buff(cor)}$ in acetate buffers against fraction base. Open circles **3-UA**, full circles **2-UA**. The line drawn shows the least-squares fit of the data for **2-UA**.

catalysis illustrated in Fig. 1. As follows from the pK_{UA} values for the dissociation of the carboxy group in the hydantoic acids listed in Table 5, partial or full conversion to the anions will take place in the remaining buffers. This has to be taken into account when the kind of general catalysis, acid or base, is determined. Thus, general acid catalysis, observed in buffers where an acid substrate is fully ionized, is accounted for by the kinetically equivalent general base catalysis of the reaction of the free acid. We found that, in the more basic formate, acetate and cacodylate buffers, only general base catalysis is significant when the rates are corrected for ionization. The behavior of the acids in these buffers is similar to that of their ethyl esters,[3] giving curved plots $k_{buff(cor)}$ against fraction base; for the acids the curvature is much more marked for the reaction of **3-UA**, as shown by the results for acetate buffers shown in Fig. 4 (the data for **2-UA** actually fit a straight line).

The relatively uncomplicated general base catalysis of the cyclization of **2-UA** was analyzed by means of a multivariable fit to eqn. (10) (as used also for the corresponding ethyl ester

$$k_{cor} = k^1_H + \frac{k_w + k_{OH}a_{OH} + k_{A^-}[A^-]}{1 + k^2_H a_H} \qquad (10)$$

in the same buffers[3]), inserting the hydrolysis rate constants derived above from the rate profile.††

†† k_{cor} are the observed rates corrected for ionization by means of eqn. (6). The constant k_{A^-} is the rate of general base catalysis by the base A^-.

The data are summarized in Table 3. The constant k^2_H, derived from the rate profile (785 dm^3 mol^{-1} s^{-1}), indicates that the denominator tends towards unity above pH 3. In cacodylate the best fit is obtained with eqn. (10), but in formate and acetate the fit is improved slightly by including a term for the catalysis of the reverse reaction by the buffer conjugate acid, k_{AH} (Scheme 2, breakdown of $\mathbf{T}^-$ to reactant), eqn. (11).

$$k_{cor} = k^1_H + \frac{k_w + k_{OH}a_{OH} + k_{A^-}[A^-]}{1 + k^2_H a_H + k_{AH}[AH]} \qquad (11)$$

The curvature of the plots (Fig. 4) of $k_{buff(cor)}$ *vs.* fraction of free base can alternatively be accounted for by the inclusion of a third-order term, as in eqn. (12), where k^A_B is the rate constant for simultaneous catalysis by the buffer base and OH^-. Eqn. (12) is applied for the case of **3-UA** being an extension of eqn. (8).

$$k_{cor} = k_H a_H + k_w + k_{OH}a_{OH} + k_{A^-}[A^-] + k^A_B a_H[A^-] \qquad (12)$$

General acid catalysis by the buffer conjugate acid of the reverse reaction (eqn. (11) and Scheme 2, breakdown of $\mathbf{T}^-$) is the most likely explanation for the curvature, both mechanistically and experimentally for the cyclizations of both the esters and of **2-UA**: because with the esters there is no plausible mechanism involving a second base; and because the curvature is more marked for more strongly acidic buffers (glycine, acid phosphate), as would be expected from a normal Brønsted dependence. However, for **3-UA** strong curvature persists in the more basic buffers (see Fig. 4), and the best fits (Table 4) were obtained using eqn. (12). This is consistent with base-catalyzed cyclization of the anion becoming important in these buffers as a parallel reaction, no doubt because of the GDME. With 2,2,3,5-tetramethylhydantoic acid, with the same pattern of substitution in the chain but a more nucleophilic ureide (ω-Me), this is the only base-catalyzed reaction observed.[10] The preferred mechanism is outlined in Scheme 3: the transition state ($\mathbf{TS}^A_{f1}$) for the rate determining k^A_{f1} step avoids the formation of the doubly negatively charged $\mathbf{T}^{2-}$.

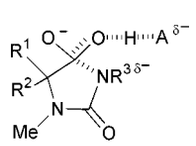

$\mathbf{TS}^A_{f1}$

Table 4 Buffer catalysis data for the cyclization of 2,2,3-dimethyl-5-(4-nitrophenyl)hydantoic acid, **3-UA**, at 25.0 °C and ionic strength 1.0 M

Buffer acid	pK_{AH} [a]	Conc. range [b]/mol dm^{-3}	Fract. base	k_{A^-}/dm^3 mol^{-1} s^{-1} [b]
$H_3N^+CH_2CO_2H$	2.45	0.009–0.185	0.242	$(6.4 \pm 1.6) \times 10^{-4}$ [c]
		0.009–0.185	0.459	
		0.009–0.185	0.675	
		0.009–0.185	0.892	
HCO_2H	3.57	0.01–0.2	0.1	0.0238 ± 0.0074 [d]
		0.01–0.2	0.3	$k_B^A = (5.99 \pm 1.18) \times 10^8$
		0.01–0.2	0.5	
		0.01–0.2	0.7	
		0.01–0.2	0.9	
CH_3CO_2H	4.62	0.009–0.178	0.215	0.202 ± 0.013 [d]
		0.009–0.178	0.44	$k_B^A = (1.42 \pm 0.19) \times 10^8$
		0.009–0.178	0.664	
		0.009–0.178	0.888	
$(CH_3)AsO_2H$	6.19	0.01–0.2	0.1	10.7 ± 1.2 [d]
		0.05–0.2	0.3	$k_B^A = (2.73 \pm 0.50) \times 10^8$
		0.05–0.2	0.5	
		0.05–0.2	0.7	
		0.05–0.2	0.9	

[a] pK_{AH} values from ref. 6. [b] Three or four runs carried out within each concentration range. [c] Approximate value. [d] Calculated from eqn. (12).

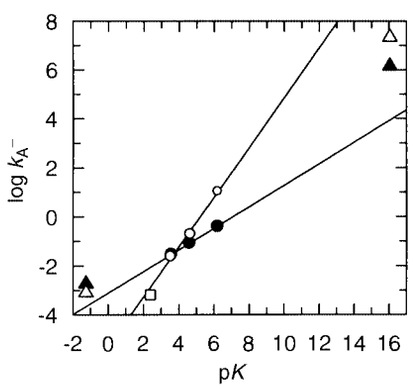

Fig. 5 Brønsted plots for the cyclization of the free ureido acids: closed symbols are for **2-UA**, open symbols for **3-UA**. Circles represent data for formate, acetate and cacodylate, triangles represent k_w and k_{OH}, and the square represents an approximate value for catalysis by glycine. The lines represent linear fits of the data for formate, acetate and cacodylate only.

Brønsted plots of the catalytic constants for the free ureido acids are shown as Fig. 5. The β values are based on the data in formate, acetate and cacodylate. The results for **2-UA** are similar to those observed with the esters of the acids **1** and **2**: the β value is 0.44 compared to values of 0.50–0.58 observed for the esters. The point for catalysis by water falls close to the line of best fit, while that for OH^- shows a large positive deviation for the specifically-catalyzed reaction. As discussed previously, this behavior is best explained by attack on the carboxy group being concerted with deprotonation of the ureido group. The normal isotope effect of k_{buff} (Table 2) is consistent with such a mechanism.

The behavior of **3-UA** is completely different, with general base catalysis characterized by a β value of 1.0 (Table 5), evidence for rate-determining diffusion-controlled proton transfer. In such cases the Brønsted plots present Eigen[11] curves which have slopes of unity when the base strength is varied in the uphill (endoergic) region. Some insight into the various reaction steps can be gained by estimating the rates of proton transfers and of cyclization of the ureide anion, using the pK for ionization of the ureido group. As discussed above, when $A^- = OH^-$ (the first step of Scheme 2), k_{f1}, is specific base-catalyzed, with the formation of $\mathbf{T}^-$ being rate determining. Thus k_{f1} can be represented as $k_{f1}^{AH}K_{UA}^{NH}/K_w$, where k_{f1}^{AH} is the rate constant for the cyclization of the ureide anion of the free acid and k_{UA}^{NH} is the dissociation constant of the ureido group in the free acid (Scheme 4).

Table 5 Brønsted β values for GBC of ureido acids, pK data, λ_{max} of ureide anion

Compound	β values	pK_{UA}	pK_{UA^-}	$\lambda_{max}^{anion\ a}$/nm
1-UA		3.52 ± 0.02	14.19 ± 0.03	454
2-UA	0.439 ± 0.007	3.60 ± 0.02	14.27 ± 0.03	458
3-UA	1.02 ± 0.06	4.22 ± 0.12 [b]	14.51 ± 0.02	470

[a] Data in 1 M KOH; a bathochromic shift is observed in more concentrated solutions. [b] From rate profile.

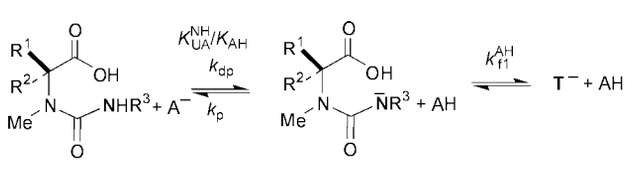

Scheme 4

At the pH of the determination, the carboxy group is, of course, ionized, and the values of pK_{UA^-} in Table 5 refer to the ureido group of the hydantoate anion. An estimate for the change in pK caused by replacing CO_2^- with CO_2H in a complex molecule like **3-UA** can only be very approximate. Viewing ArNHCO as equivalent to a carboxy group we can use as a model succinic acid, for which ΔpK between the two carboxy groups is 0.69.‡‡ Correcting the measured pK_{UA^-} by this amount gives§§ $k_{UA}^{NH} = 1.45 \times 10^7$ and 5.5×10^5 s^{-1} for the cyclization of the ureide anion of **3-UA** and for the corresponding reaction of **2-UA**, respectively. Although the estimated rate difference is only 26-fold, this is probably the most important factor accounting for the different mechanisms for general base catalysis of the two hydantoic acids. In the alternate route interpretation[12] for a concerted process (deprotonation of the ureido group and cyclization of the anion in the present case) both processes must have similar barriers for the route to products to lie along a diagonal reaction coordinate. Apparently the cyclization of the anion of **3-UA** has become sufficiently rapid for the two steps to proceed consecutively, deprotonation becoming rate determining. The steady state

‡‡ Statistically corrected; from R. Steward, *The Proton: Applications to Organic Chemistry*, Academic Press, New York, 1985, p. 35.
§§ $pK_w = 14$ was used because acidity functions give thermodynamic pK values.

approximation with respect to the ureide anion $\mathbf{N}^-$ of Scheme 4 gives eqn. (13).

$$k_{f1} = \frac{V}{[\mathbf{UA}][A^-]} = \frac{k_{dp}k_{f1}^{AH}}{k_p[AH] + k_{f1}^{AH}} \qquad (13)$$

The constants are defined in Scheme 4, k_p is the rate of protonation of $\mathbf{N}^-$, k_{dp} is the rate of deprotonation of **UA**, k_{f1}^{AH} is the rate of cyclization of the anion $\mathbf{N}^-$ (k_{f1} of Scheme 2 groups deprotonation and cyclization into one apparent process). For deprotonation to be rate-determining, the condition $k_p[AH] < k_{f1}^{AH}$ should apply. With the buffer acids studied, k_p should be diffusion controlled: it can be estimated from the equilibrium of the first step, eqn. (14).

$$k_{dp} = k_p \frac{K_{UA}^{NH}}{K_{AH}} \qquad (14)$$

Using $pK_{UA}^{NH} = 13.83$ and the thermodynamic values §§ for K_{AH}, a value for k_p of $(2.9 \pm 0.6) \times 10^8$ dm^{-3} mol^{-1} s^{-1} is calculated, based on the rate constants for GBC in Table 4. This value is somewhat lower than the usual range of 10^9–10^{10} for a diffusion-controlled process, but this is not unexpected[13] in view of the steric shielding of 5-N in the most likely (3*E*,4*Z*) rotamer of the ureide group in the anion **3-N**$^-$.

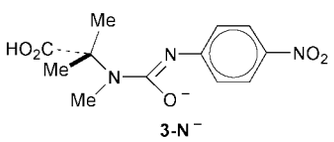

3-N$^-$

Although the estimate of k_p is about 20 times larger than that of k_{f1}^{AH}, the two terms $k_p[AH]$ and k_{f1}^{AH} in the denominator of eqn. (13) will be more or less equal at a typical buffer ratio ($[A^-]$/[AH]) of 1 and concentration of buffer = 0.1 M (Table 4). Bearing in mind the uncertainties involved, one of which is the implicit assumption that the differences in p*K* values (and K_w) remain the same upon changing the ionic strength from zero to 1, these estimates support our conclusion above, that $k_p[AH] < k_{f1}^{AH}$ for the GBC observed with **3-UA** (the inequality need not be large). On the other hand, specific base catalysis for the reaction catalyzed by OH^- demands the alternate inequality $k_p[AH] > k_{f1}^{AH}$. In this case AH is H_2O and k_p should be considerably greater because of its size and the Grotthuss mechanism involving proton jumps along a hydrogen bonded network of water molecules. This makes the change in mechanism from GBC to SBC understandable.

Discussion

The *gem*-dimethyl effect

This study has shown that a normal GDME operates in the cyclization of the ureido-acid **3-UA**, which reacts 15 times faster than **2-UA**. The disappearance of the GDME observed for the cyclizations of esters of ω-methyl, phenyl or *p*-nitrophenyl-ureido **3-UA** is evidently a function of the esterifying group. This result is consistent with our interpretation in terms of steric hindrance to protonation of the departing ester ethoxy group: replacing ethyl by hydrogen opens a path of easy approach to the general acid.

There is a delicate balance between the various mechanisms observed in the cyclization of the ω-(*p*-nitrophenyl)hydantoic acids studied in this work and the way the GDME affects the balance between them. The GDME results mainly from steric strain, the substituents introducing more strain in the open chain than in the ring compound because bonds are forced into unfavourable comformations or geometries in the ring, thus allowing more freedom for the substituents. Although steric effects often defy quantitative correlations such as linear free energy relationships, we have shown previously[14] that the *gem*-dimethyl effect does obey Leffler-type relationships in some cases [eqn. (15)].

$$\log (k_X/k_O) = a \log (K_X/K_O) \qquad (15)$$

Here k_X are the rate constants and K_X the equilibrium constants for the same reaction. The *a* values observed can be related to the position of the transition state on the reaction coordinate. Qualitatively, a tight transition state will lead to a relatively large GDME, and *vice versa*. Many examples have been identified by one of us.[15] In reactions of the type studied in this paper, where a relatively rigid ring system is formed *via* a tetrahedral intermediate, flexibility is gradually lost along the reaction coordinate from reactant to product. Consistent with this expectation $K_e(\mathbf{3})/K_e(\mathbf{2}) = 2800$ (670 when recalculated for the neutral species **[H]** and **[UA]**). This ratio is much higher than observed for the rate constants; $k_H(\mathbf{3})/k_H(\mathbf{2}) = 47$ and $k_{OH}(\mathbf{3})/k_{OH}^b(\mathbf{2}) = 15$. Earlier work[3,16] suggested that the acid-catalyzed reaction involves rate-determining formation of the tetrahedral intermediate. Here the constants k_{OH} also refer to the first cyclization step (k_{f1} of Scheme 2).

We can rationalize the observed changes in mechanism on the basis[4] that the GDME will tend to shift the rate-determining transition state to an earlier step by favouring the forward *vs.* the reverse reactions, thus changing the partitioning ratio of the intermediate. This consequence of the general GDME explains why the OH^--catalyzed reaction observed at lowest pH with **2-UA** is not detected with **3-UA**. For this reaction the departure of OH^- is rate limiting and $k_{r1H} > k_{f2H}$. With **3-UA** this inequality is apparently reversed and the change of mechanism is no longer observed.

Two other changes of mechanism due to the action of GDME were already noted in the Results section. The first concerns the appearance of the reaction of the carboxylate anion, followed by a rapid change in rate determining step from the addition of the ureido group to the departure of the hydroxide ion. In the reverse reaction, the hydrolysis of hydantoins, equivalent second order terms in $[OH^-]$ and a change in mechanism have often been observed, and assigned[17] as catalysis through $\mathbf{T}^{2-}$. This reaction is exhibited by hydantoins as well as the six-membered dihydrouracils[18] bearing H or alkyl at N(3). When the substituent is changed to aryl only a first order reaction in $[OH^-]$ is observed, with evidence consistent with this being a rate determining attack of hydroxide ion on the hydantoin.[19] This was readily rationalized in terms of the improved leaving ability of the arylureido group. The involvement of a second order term in $[OH^-]$ (based on the reaction of free acid) in the cyclization of **3-UA** is thus an example of how the GDME acts to increase nucleophilicity.

The second point of note is the changeover from a concerted to a step-wise mechanism of GBC on going from **2-UA** to **3-UA** and how these compare with the mechanisms observed with the esters. We found before, in the case of ω-methyl- or phenyl-hydantoic esters,[2] that the intramolecular attack of the ureide anions is a very fast reaction (rate constant of the order of 10^8 s^{-1}), and pointed out that the activation energies concerned are comparable to the barriers for rotation within the ureido group needed for the reaction to take place. This argument explained the insensitivity towards electronic effects (Me *vs.* Ph) of the reactivity of the anions. Recent reports[3] of reactions of ω-(*p*-nitrophenyl)hydantoates gave values for k_{OH} of the order of 5×10^6 dm^3 mol^{-1} s^{-1}, which should be more or less equal to those of their anions according to the p*K* of 14 reported for *p*-nitrophenylurea. These values proved sufficiently high for a hindered proton transfer to the leaving group to become rate limiting in the ester of **3-UA,** the second step in Scheme 2. The study of these esters showed also that GBC with the fully methylated ester of **3-UA** involves proton donation to the

leaving EtO^-, while with esters of **2-UA** abstraction of the NH proton by the general bases, concerted with formation of $\mathbf{T}^-$, is rate determining. In the less hindered free acid **3-UA** the rate constant for cyclization of the anion was estimated above as 1.45×10^7 s^{-1} but despite this higher value the first step of Scheme 2 remains rate limiting as with **2-UA**. The above analysis of the steady-state solution of this process (eqn. (13)) gives a reasonable explanation for the two different rate determining stages in the formation of $\mathbf{T}^-$. Because of the much smaller value of k_{f1}^{AH} with **2-UA**, this analysis predicts SBC cyclization of the anion to be rate determining. Instead, the system chooses a different pathway. a concerted GBC reaction. This avoids formation of $\mathbf{T}^{\pm}$ in the presence of general bases but is rendered unnecessary in **3-UA** by the GDME, which results in one of the alternate routes becoming the lowest energy path.

The diversity of mechanisms observed in the hydantoic acid systems reported in this and our preceding papers[2,3,16] underlines the need for caution in extrapolating results from even very simple model systems, particularly to more complex situations.

Acknowledgements

We thank the National Foundation for Scientific Research of Bulgaria for funding this research, the Royal Society for travel funds and the Royal Society of Chemistry for a Journals Grant for International Authors (to IGP).

References

1 C. K. Ingold, *J. Chem. Soc.*, 1921, **119**, 305; C. K. Ingold, S. Sako and J. F. Thorpe, *J. Chem. Soc.*, 1922, 1117; N. L. Allinger and V. Zalkow, *J. Org. Chem.*, 1960, **25**, 701; I. B. Blagoeva, B. J. Kurtev and I. G. Pojarlieff, *J. Chem. Soc.*, *Perkin Trans. 2.*, 1979, 1115; A. J. Kirby, *Adv. Phys. Org. Chem.*, 1980, **17**, 183; R. E. Valter, *Usp. Khim.*, 1982, **51**, 1374; L. Mandolini, *Adv. Phys. Org. Chem.*, 1986, **22**, 17; S. P. Verevkin, M. Kümmerlin, H.-D. Beckhaus, C. Galli and C. Rüchardt, *Eur. J. Org. Chem.*, 1998, 579.
2 E. Atay, I. B. Blagoeva, A. J. Kirby and I. G. Pojarlieff, *J. Chem. Soc.*, *Perkin Trans. 2*, 1998, 2289.
3 I. B. Blagoeva, A. J. Kirby, A. H. Koedjikov and I. G. Pojarlieff, *Can. J. Chem.*, 1999, **77**, 849.
4 A. H. Koedjikov, I. B. Blagoeva, I. G. Pojarlieff and A. J. Kirby, *J. Chem. Soc.*, *Perkin Trans. 2*, 1996 2479.
5 A. K. Covington, R. A. Robinson and R. G. Bates, *J. Phys. Chem.*, 1966, **70**, 3820; J. C. Fishbein and W. P. Jencks, *J. Am. Chem. Soc.*, 1988, **110**, 5075.
6 I. B. Blagoeva, *J. Chem. Soc.*, *Perkin Trans. 2*, 1987, 127.
7 I. B. Blagoeva, A. H. Koedjikov, I. G. Pojarlieff and M. M. Toteva, *Dokl. Bolg. Akad. Nauk*, 2000, **53**, No. 10, 33.
8 G. Yagil, *J. Phys. Chem.*, 1967, **71**, 1034.
9 L. Schowen, *Prog. Phys. Org. Chem.*, 1972, **9,** 275.
10 I. B. Blagoeva, I. G. Pojarlieff and A. J. Kirby, *J. Chem. Soc.*, *Perkin Trans. 2*, 1984, 745.
11 M. Eigen, *Angew. Chem. Int.*, *Ed. Engl.*, 1964, **3**, 1.
12 R. A. More O'Ferrall, *J. Chem. Soc. B*, 1970, 274; W. P. Jencks, *Chem. Rev.*, 1972, **72**, 702.
13 J. R. Keeffe and A. J. Kresge, in *Investigation of Rates and Mechanisms of Reactions*, *Vol. 6*, *Part 1*, ed. C. F. Bernasconi, John Wiley, New York, 1986, p. 752; F. Hibbert. *Adv. Phys. Org. Chem.*, 1986, **22**, 113; J. P. Guthrie, J. Cossar and A. Klym, *J. Am. Chem. Soc.*, 1984, **106**, 1351.
14 I. B. Blagoeva, I. G. Pojarlieff and V. I. Rachina, *J. Chem. Soc.*, *Chem. Commun.*, 1986, 946.
15 A. J. Kirby, *Adv. Phys. Org. Chem.*, 1980, **17**, 183.
16 E. Atay, I. B. Blagoeva and I. G. Pojarlieff, *Dokl. Bolg. Akad. Nauk*, 2000, **53**, No. 2, 61.
17 I. B. Blagoeva, I. G. Pojarlieff and V. S. Dimitrov, *J. Chem. Soc.*, *Perkin Trans. 2*, 1978, 887.
18 E. G. Sander, *J. Am. Chem. Soc.*, 1969, **91**, 3629; I. B. Blagoeva, B. J. Kurtev and I. G. Pojarlieff, *J. Chem. Soc. B*, 1970, 232.
19 I. B. Blagoeva and I. G. Pojarlieff, *Dokl. Bolg. Akad. Nauk*, 1977, **30**, 1043; M. Bergon and J.-P. Calmon, *J. Chem. Soc.*, *Perkin Trans. 2*, 1978, 493.
20 J. Kavalek, V. Sterba and S. El Bahaie, *Collect. Czech. Chem. Commun.*, 1983, **48**, 1753.